

Narrow-linewidth semiconductor laser with highly-linear frequency modulation response for coherent sensing

Vincent Cardin, Daniel Robin, Sylvain Boudreau, Guy Rousseau, Simon Ayotte*, Marie-Claude Vallières Riendeau, Patrick Larochelle, François Costin, Émile Girard-Deschênes, Philippe Chrétien, Guillaume Brochu, Patrick Dufour, Sébastien Deschênes, Katherine Légaré, Mathieu Faucher
TeraXion, 2716 rue Einstein, Québec, Québec, Canada G1P 4S8

Mohamed Rahim, Grzegorz Pakulski, Muhammad Mohsin, Darren Goodchild, Philip Waldron, Bernard Paquette, Omid Salehzadeh Einabad, Daniel Poitras
National Research Council of Canada, 1200, Montreal Road, Ottawa, Ontario, Canada K1A 0R6

ABSTRACT

A narrow-linewidth semiconductor laser chip with highly linear frequency modulation response is presented and validated in two coherent sensing test experiments. This distributed feedback laser monolithic chip has an intrinsic linewidth of less than 10 kHz and an output power over 60 mW. When its injection current is modulated by a triangular function, the laser optical frequency can be modulated by more than 7 GHz at rates up to 100 kHz. The laser frequency modulation response is extremely flat up to 100 MHz, which allows correcting the residual sweep nonlinearities by a proper pre-distortion of the modulation signal. In a first test experiment, the laser was used into a monostatic FMCW lidar system. A point cloud was acquired with a field of view of 20°(H) x 10°(V) and an angular resolution of 0.05° along both axes. The acquisition was performed without averaging using a 7 mm diameter output beam of 100 mW. A high-quality point cloud including several objects of varying reflectivity was measured. In a second test experiment, the laser was used into an OFDR system for a distributed acoustic sensing (DAS) experiment. A short portion of a 50 m long SMF-28 fiber was exposed to a 2 kHz acoustic signal. Processed data clearly shows a strong 2 kHz tone at the location of the acoustic perturbation. In both test experiments, the laser was successfully linearized using modulation signal pre-distortion based on interferograms obtained with a Mach-Zehnder interferometer.

Keywords: Narrow linewidth laser, Semiconductor laser, Linear frequency modulation, FMCW lidar, Optical Frequency Domain Reflectometry, Distributed acoustic sensing, Coherent sensing.

1. INTRODUCTION

Narrow-linewidth lasers have proven to be instrumental in the emergence of a variety of phase sensitive sensing applications. In the vast field of coherent sensing applications, where a local oscillator is used in the acquisition chain, the level of frequency noise of the laser source is often a limiting factor in reaching high system performance. Distributed acoustic sensing (DAS) systems [1] rely on ultra-narrow-linewidth lasers to achieve system range up to a hundred kilometers with minimal impact on the distance resolution. Depending on the application and system architecture, one may also benefit from modulating the laser frequency to extract positioning and doppler information, as it is the case in frequency modulated continuous wave (FMCW) lidar [2]. Frequency modulation of narrow linewidth laser sources is also beneficial to reach high spatial resolution in fiber sensing systems based on Rayleigh scattering to perform strain, temperature, and vibration measurements [1]. Additional applications include biosensing [3] and fiber optic rotation sensing [4]. Here we demonstrate an intrinsically narrow-linewidth semiconductor distributed feedback (DFB) laser diode design that combines low phase noise with unique frequency modulation (FM) properties, which are key enablers for the emergence of lower cost coherent sensing systems.

2. PERFORMANCE OF THE LASER

2.1 Small-signal frequency response

The complex FM response of a laser is critical for multiple aspects of sensing. Having a well-behaved response, that is flat in both amplitude and phase up to very high frequencies, enables the use of feedback loops that can reduce the frequency noise of the laser by several orders of magnitude. Good FM response is also useful in the context of FMCW-based sensing,

* sayotte@teraxion.com; phone 1-418-658-9500 ext. 482

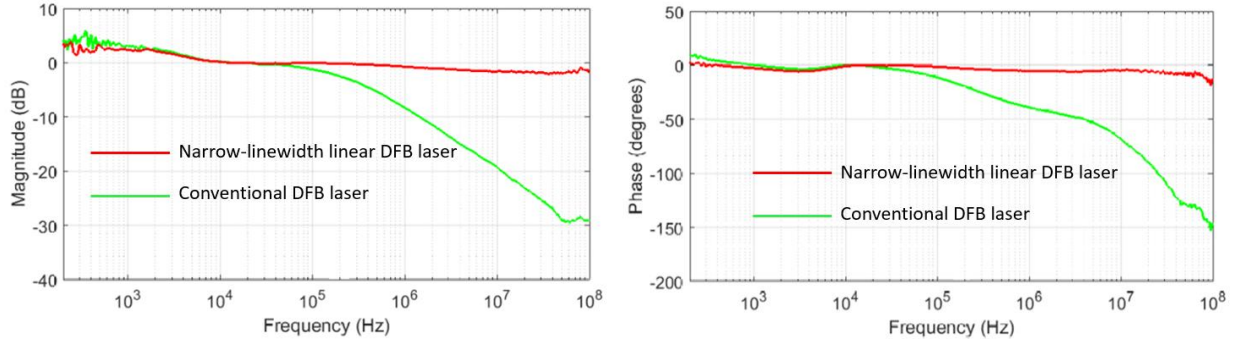


Figure 1 : Comparison of the small signal FM response of our custom DFB laser to that of a conventional DFB laser.

where linear frequency ramps are generated, and where nonlinearities in the sweeps generate distortions that reduce the resolution and the sensitivity of the system. In this case, having a good FM response can help correct the sweep nonlinearities by pre-distorting the modulation signal.

In a semiconductor laser, both temperature and carrier density affect the index of refraction. Whereas an increase in temperature leads to a larger index of refraction, an increase in carrier density leads to a reduced index of refraction. The thermal effect dominates at low frequencies but has a limited bandwidth of about 100 kHz while the carrier density effect remains flat up to many GHz and typically has the opposite sign. This explains the typical FM response of a DFB laser. Our laser was specifically engineered to have a flat FM response by forcing their charge-carrier-based and thermal components to have the same sign, which greatly reduces large magnitude drops and phase shifts that typically occur above 100 kHz in conventional DFB lasers. Figure 1 shows the difference between our DFB and a conventional DFB laser. Our laser exhibits flat response, both in frequency and phase, whereas the conventional DFB laser starts rolling off between 100 kHz and 1 MHz.

2.2 Intrinsic and stabilized frequency noise

The frequency noise of a laser is a very important performance metric for coherent sensing applications, since it is related to its coherence length, and thus determines the range at which coherent sensing can be successfully performed. For white frequency noise, the coherence length L_{coh} is given by $L_{coh} = c/\pi^2 \text{PSDFN}$, where c is the speed of light, and PSDFN is the power spectral density of the frequency noise of the laser.

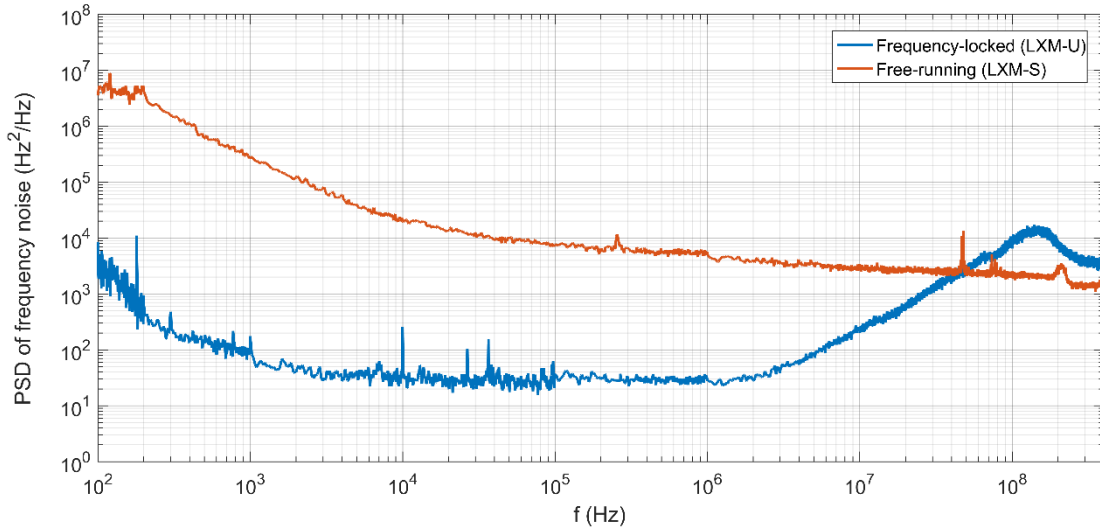


Figure 2 : Native and frequency-locked PSD of frequency noise of the laser.

Figure 2 shows the PSDFN of our laser in two different configurations. In the free-running configuration, the high frequency, flat section of the PSDFN, that corresponds to the so-called short-term linewidth, has a value of approximately $3000 \text{ Hz}^2/\text{Hz}$. This corresponds to a linewidth of 10 kHz, and to a free-space coherence length of about 10 km, or a round-trip fiber coherence length of $\sim 3 \text{ km}$. For applications that require even longer coherence lengths, the aforementioned flat FM response enables the laser to be frequency-locked to a frequency discriminator [5], which reduces the frequency noise up to a few orders of magnitude at tens of MHz. This is shown on the blue curve of Figure 2, where the PSDFN bottoms out at a value of $25 \text{ Hz}^2/\text{Hz}$ between 5 kHz and 2 MHz.

2.3 Large signal frequency modulation and linearizability

For FMCW sensing applications, the combination of high ramp rates (for high measurement rates), high frequency excursion (for high spatial resolution), and low linearity residuals (for high spatial resolution, high signal-to-noise ratio, and range precision), can be challenging. Our laser, thanks to its flat frequency response, can be easily linearized at ramp rates up to 100s of kHz using pre-distortion of the driving signal.

To linearize the laser, its instantaneous optical frequency profile must be measured. To that end, the laser beam was launched into an all-fiber Mach-Zehnder interferometer producing the beating of two copies of the laser output delayed relatively by a time determined by the length mismatch between the arms of the interferometer. The time variation of the optical frequency is determined by analyzing the power beats at the output of the interferometer [6].

In a first experiment, we modulate a laser with a frequency excursion amplitude of 2 GHz at a repetition rate of 100 kHz with $5 \mu\text{s}$ up and down ramps. The upper graphs of Figure 3 show the instantaneous optical frequency versus time when the laser injection current is driven with the pre-distorted signal of Figure 4 or with a pure triangular signal. The lower graphs show the residual non-linearity of both cases. The standard deviation of the non-linearity without pre-distortion is 47 MHz (2.4%) and with pre-distortion, it is improved by 100 and goes down to 0.5 MHz (0.02%). The peak-to-peak error of the non-linearity without pre-distortion sits at 190 MHz (9.5%) and with pre-distortion, it goes down to 2.5 MHz (0.13%).

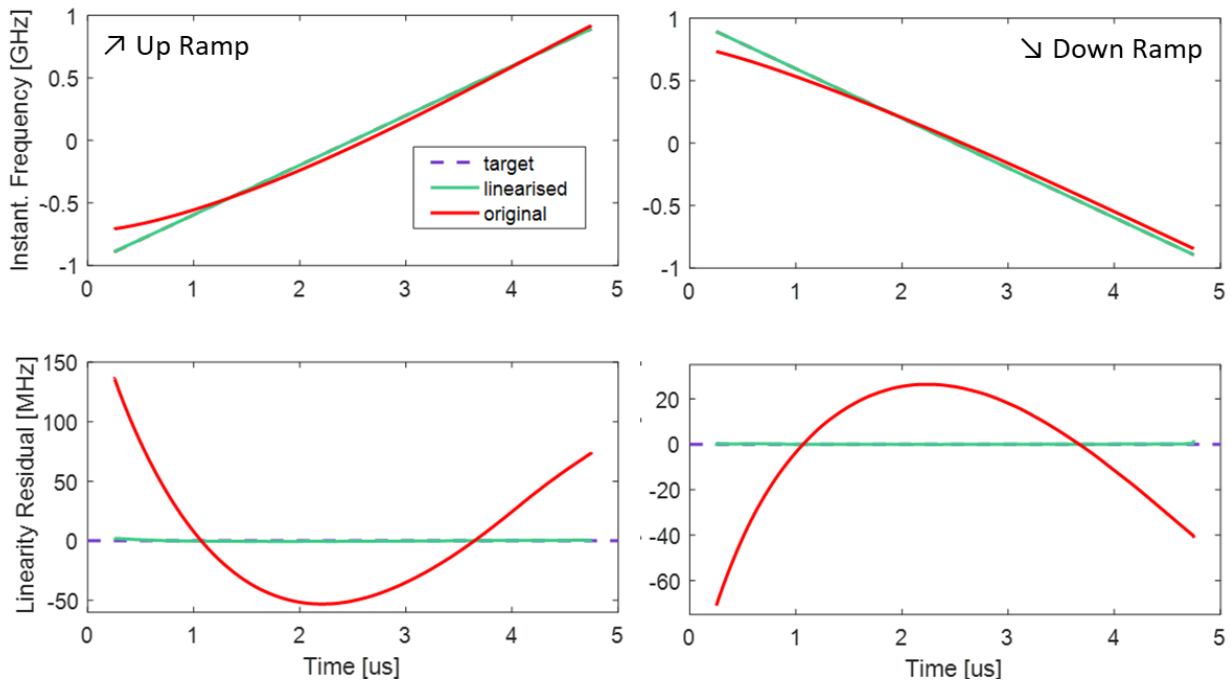


Figure 3 : Triangular frequency modulation with and without pre-distortion signal. Upper images show the instantaneous optical frequency for the up and down ramp, and lower graphs show the residual non-linearity.

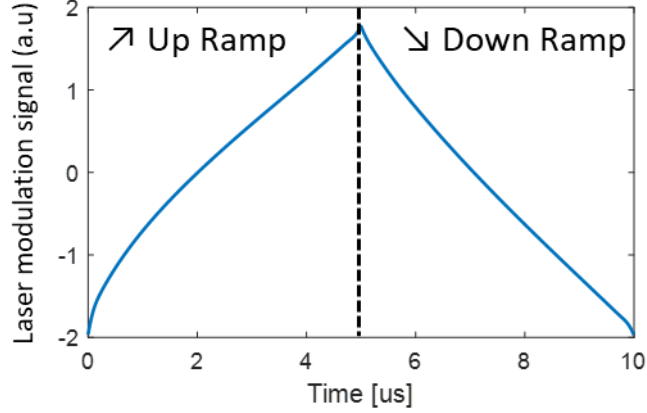


Figure 4 : Pre-distorsion signal used to modulate the laser current and obtain linear optical frequency.

In a second experiment, the laser frequency excursion amplitude is pushed to 7.5 GHz. The initial drive signal at repetition rate of 10 kHz is perfectly triangular, corresponding to $k = 0$ on Figure 5. As shown on the right graph of Figure 5, this baseline case corresponds to a nonlinear residual frequency nonlinearity of ± 100 MHz. Correction profiles were then iteratively applied. After two iterations ($k = 1$ and 2), the standard deviation of the nonlinear residual was brought down to 3 MHz, corresponding to 0.04% of the frequency excursion over 90% of a half-period of the modulation.

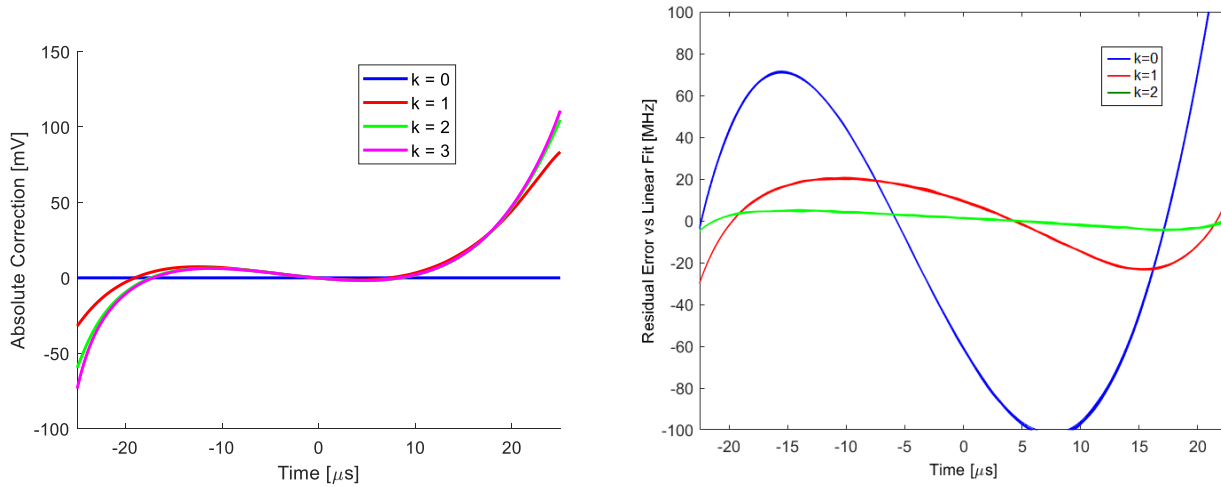


Figure 5 : Iterative correction of the modulation signal to linearize the optical frequency. The third correction was not applied.

3. APPLICATION DEMONSTRATIONS

An FMCW lidar experiment was carried out using our laser. The laser was amplified to 100 mW using a semiconductor optical amplifier. The triangular modulation period was 10.24 us (repetition rate of 97.66 kHz). The frequency modulation span was 1 GHz pk-pk. The optical system was a monostatic configuration with a collimator effective focal length of 25.49 mm at 1.55 um (TC25APC-1550 from Thorlabs). The output beam diameter (99%-energy) was 7 mm. We used a 10 mm clear aperture 2D galvanometer scanner (ScannerMax Saturn 9B). The field of view was $20^\circ(\text{H}) \times 10^\circ(\text{V})$ with angular resolution of 0.05° along both axes. The total number of points was thus 400 pts x 200 pts = 80 kpts. The acquisition was performed without averaging in (slow) “point and shoot” mode, but the acquired data corresponds to a total acquisition time of 0.8192 s. Figure 6 shows a point cloud including several objects of varying reflectivity at distances ranging from 6 m to 26 m. On the left side of the image, a range color code is used, whereas a reflectivity color code is used for the right side.

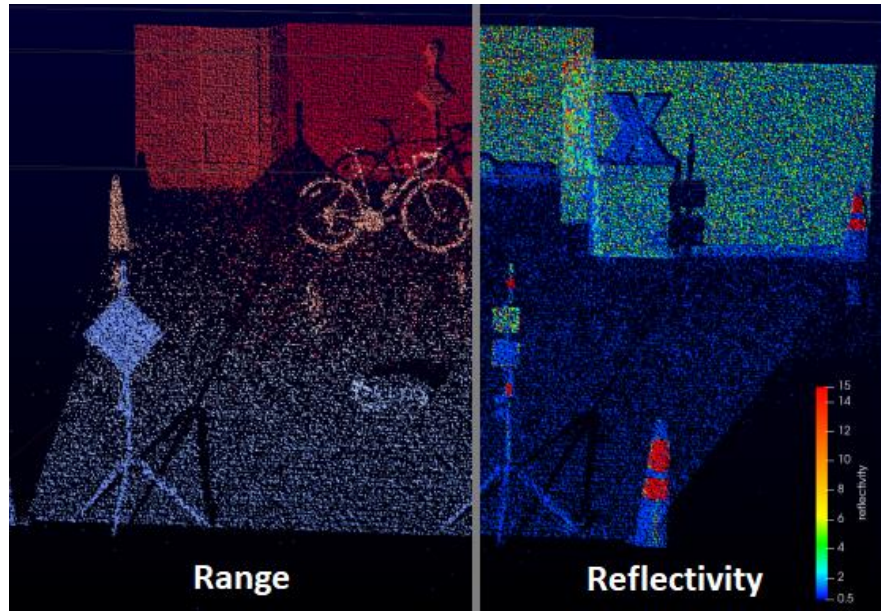


Figure 6 : Point cloud of a scene containing targets at multiple distances, sizes and reflectivity. Points are colored according to range on the left, and reflectivity on the right.

As another application of the laser, an OFDR-based DAS experiments was carried out. A short portion of a 50 m spool of SMF-28 fiber was exposed at 17 m from the optical injection point, so that a 2 kHz sinusoidal acoustic signal could be injected by making contact between a small speaker and the coating of the fiber. The probing and detection scheme is very similar to the lidar experiment, with the exception that the laser signal is injected inside the fiber rather than collimated in free space.

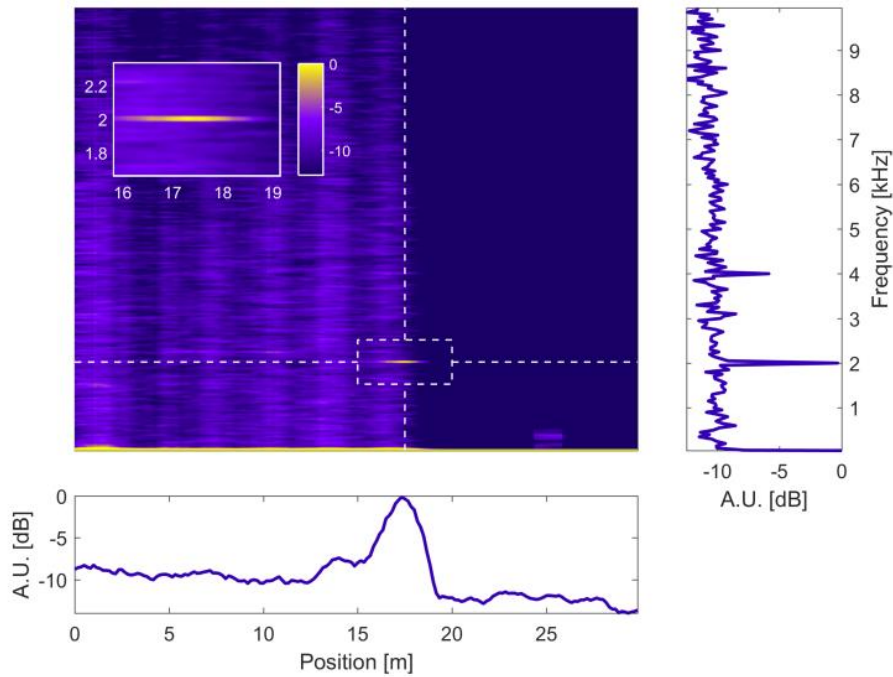


Figure 7 : DAS map inside the 50 m fiber spool, truncated between 0 m and 30 m. The signature of the 2 kHz signal that was injected at 17 m can be seen on the map and on the spectral and position slices around the point of interest.

As the raw detected signal is a single interference signal as a function of time, several steps need to be taken to generate such an image. First, the time-domain trace is sliced into a 2D matrix, where each line corresponds to a single ramp of the FMCW signal. Next, a Fourier transform is taken in the dimension of the ramp to generate a distance representation of each line, as is typical in FMCW processing [2]. At this point, each line represents the state of the Rayleigh backscattering behaviour of the fiber at different moments in time, spaced by the inverse of the ramp repetition rate. Finally, a Fourier transform is taken along the columns, so that vertical slices represent the acoustic spectrum at the corresponding distance inside the fiber. Figure 7 shows the acoustic frequency spectrum as a function of distance inside the fiber. The injected signal is strongly localized at 17 m and 2 kHz, as can clearly be seen on the acoustic frequency and position slices.

4. CONCLUSION

A semiconductor laser with a linewidth below 10 kHz, and high bandwidth FM response has been demonstrated. Its optical frequency linearity, as well as its frequency noise, can be further enhanced by electronic pre-distortion of the modulation signal. Application examples in lidar and fiber sensing were shown.

ACKNOWLEDGEMENTS

TeraXion acknowledges the financial support of the National Research Council of Canada Industrial Research Assistance Program (NRC IRAP).

REFERENCES

- [1] Gagliardi, G. et al., "Optical Fiber Sensing Based on Reflection Laser Spectroscopy," *Sensors* 10, 1823-1845 (2010).
- [2] Pierrottet, D. et al., "Development of an All-Fiber Coherent Laser Radar for Precision Range and Velocity Measurements," *MRS online Proceedings* 883, PROC-883-FF2.3 (2005).
- [3] Swaim, J. D. et al., "Detection of nanoparticles with a frequency locked whispering gallery mode microresonator," *Appl. Phys. Lett.* 102, 183106 (2013).
- [4] Sanders, G. A. et al., "Development of compact resonator fiber optic gyroscopes," *IEEE Int. Symposium on Inertial Sensors and Systems* (2017).
- [5] Cliche, J.-F., Allard, M., and Têtu, M., "High-power and ultranarrow DFB laser: the effect of linewidth reduction systems on coherence length and interferometer noise," *Proc. SPIE* 6216, 62160C (2006).
- [6] M. Takeda, H. Ina, and S. Kobayashi, "Fourier-transform method of fringe-pattern analysis for computer-based topography and interferometry," *JOSA* 72, pp. 156-160 (1982).